

## REVIEW AND PROSPECTS OF RENAULT'S MPC BASED MOTION CUEING ALGORITHM FOR DRIVING SIMULATOR

Zhou FANG<sup>1</sup>, Andras KEMENY<sup>1</sup>

(1): RENAULT, Virtual Reality and Immersive Simulation Center  
TCR AVA 0 13, 1 avenue du Golf,  
78288 Guyancourt, France  
[zhou.fang@renault.com](mailto:zhou.fang@renault.com), [andras.kemeny@renault.com](mailto:andras.kemeny@renault.com)

**Abstract** – In recent years, MPC algorithm as a new method has been successfully applied for the design of motion cueing algorithm. By using an adequate formulation of MPC model and an efficient QP solver, the MPC algorithm can provide better motion restitution results than the more conventional algorithms. However, few papers give a description in detail of the used MPC technique together with the right tuning parameters. Furthermore, the algorithm's stability condition is hardly addressed in motion cueing algorithm design, except a small number of studies where generally a quasi-zero terminal set condition was applied. It is probably less critical for driving simulators without large motion platform, but it can be a crucial safety factor to consider for high performance driving simulators where the motion velocity and acceleration can be high. In this paper, we summarize the most important works on the MPC based motion cueing algorithm, including the tuning experiences.

**Key words:** MPC, motion cueing algorithm, driving simulation, driver perception, washout.

### 1. Introduction

MPC algorithm, as an important advanced control technique was proposed by the end of 70s by Richalet et al., Cutler and Ramaker respectively. Thereafter, during about ten years, it was the most important control research topic. Nowadays, it becomes one of the most popular modern control methods both in academy and industry, with an exponential increase of publications from 1995 [Sor1]. In the driving

simulation field, Dagdelen et al. [Dag1](2004) proposed a first MPC based motion cueing algorithm to optimize 1DOF motion cues with acceleration threshold control in washout process. Then we proposed an explicit MPC algorithm [Fan1] where an efficient stability condition was proposed. Augusto [Aug1], Beghi et al. [Beg1] and Al Qaisi et al. [Alq1] published the MPC algorithm using human vestibular model. Garrett et al. [Gar1](2013) published their MPC work taking into account vestibular model and hexapod constraints. Compared with that of more conventional motion cueing algorithms, such as classical, LQR optimal filters, the MPC technique reveals several potential advantages. However, by authors' experiences, different conclusions could be reached according to the cost function expression, the adopted stability condition, the weighting matrices and the predictive step length. It is worth to make some investigations to these sensible factors. This is the main motivation for the current paper.

In this paper, we have reviewed our MPC algorithm experiences and presented its prospects for future developments. A robust stability condition which can influence significantly the motion cueing results is addressed. The potential benefits to use vestibular model, the algorithm's tuning technique and in-line pre-position strategy are also investigated. Finally, diverse simulators performances are evaluated by using the proposed MPC-MCA (motion cueing algorithm).

## 2. MPC’s formulation and stability condition

A complete formulation of MPC-MCA is given in reference [Fan3]. In MPC algorithm, the cost function can be written by means of following basic formulation:

$$J_N(X_k) = \min_{u_0, u_1, \dots, u_{N-1}} \sum_{i=0}^{N-1} \|\phi_i \hat{x}_i - r_i\|_{q_i}^2 + \sum_{i=0}^{N-1} \|\Delta u_i\|_{R_u}^2 + \sum_{i=0}^{N-1} \|\hat{x}_i\|_{Q_x}^2 + \|\hat{x}_N\|_{Q_N}^2 \quad (1)$$

subject to:

$$\begin{aligned} \hat{x}_k &= A \cdot \hat{x}_{k-1} + B \cdot u_{k-1} \\ \text{constraints : } H_x \cdot \hat{x}_k + H_u \cdot u_k &\leq K \\ \text{stability constraints : } \hat{x}_N &\in \Omega \end{aligned} \quad (2)$$

where  $\hat{x}_k$  is an augmented state vector including motion perceived variables and simulated vehicle’s acceleration. The vector,  $\phi_i$ , is for extracting the corresponding motion feeling variable from  $\hat{x}_k$ .  $\Delta u$  is the linear or tilt acceleration input vector in differential form given by:  $\Delta u_{k-1} = u_k - u_{k-1}$ .  $\hat{x}_N$  is the last terminal state, introduced for algorithm’s stability consideration.  $\Omega$  is a positively invariant set. The weighting coefficient or matrices,  $q_y$ ,  $R_u$ ,  $Q_x$ ,  $Q_N$  are used to balance the trade-off between reproducing the vehicle’s dynamic motion and using simulator’s workspace, velocity and acceleration within its bounds.

In MPC-MCA, the cost function minimisation is generally subject to a linear system with input, output and state constraints. The system can be an ideal driving simulator, i.e. a double integrator, a simulator’s transfer function, or a simulator model incorporated with human vestibular one. The macroscopic algorithm’s scheme is very similar to that of LQR optimal filter, as illustrated by figure 1.

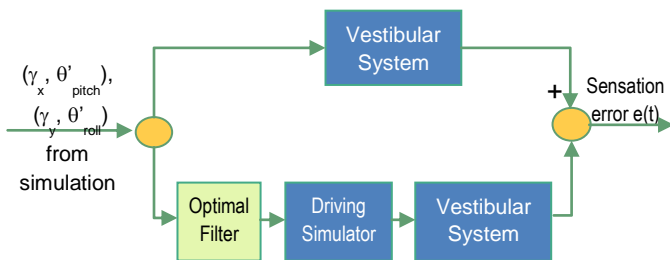


Fig. 1: LQR based motion cueing algorithm [Siv1, Tel1]

For the MPC approach, the optimal filter is replaced by MPC optimizer which minimizes the error of sensation produced from between vehicle and simulator at each time step. Generally, in motion cueing algorithm design, the actuator’s motion control system provided by manufacturer is assumed perfect and without delay. Based on this hypothesis, the system model is actually an accurate numerical model. The offset problem encountered in a real plant control due to model-plant mismatch or disturbances will disappear. Thus, the algorithm’s formulation can be reduced to its simplest expression. If the simulator’s actuator delay is important, the induced mismatch between visual, acoustic and motion sensor cues can generate the occurrence of motion sickness [Oma1]. In this case, it is necessary to compensate the delay in motion cueing algorithm design. As we reported [Fan4], it is possible to reduce this delay by using only the identified simulator transfer function. In our approach, the plant model is always a pure numerical model for the reasons of simplicity and the cost for extensive hardware modifications. Actually, we have developed a MPC algorithm to correct this delay. The feedback from the professional drivers who are very sensitive to the phase lag confirms the significant improvement of driving perception, even with a low frequency 0.2Hz slalom scenario. Later, we will present this work. The vestibular system, situated in inner ear, consists of two important parts. One contains the semicircular canals that sense rotational motion and the other, the otoliths that sense linear motion. Numerous vestibular transfer functions are presented in detail by Zacharias, Telban et al. [Tel1]. One of the typical transfer functions proposed by Young and Meiry(1968) describing the relationship between the specific force,  $f$ , and the perceived force,  $\hat{f}$ , is:

$$G_{oto}(s) = \frac{\hat{f}}{f} = \frac{k(\tau_a \cdot s + 1)}{(\tau_L \cdot s + 1)(\tau_s \cdot s + 1)}$$

The semicircular canal sensation model is given as (Young & Oman 1969):

$$G_{scc}(s) = \frac{\hat{\omega}}{\omega} = \frac{k_{scc} T_L T_a \cdot s^2}{(T_L \cdot s + 1)(T_s \cdot s + 1)(T_a \cdot s + 1)}$$

The corresponding state-space model can be written in different forms according to the tilt variable to consider in input of system, e.g.  $\theta$  for Siven et al. [Siv1],  $\omega$  for Telban et al. [Tel1]

and Chen et al. [Che1]. We give below the formulation of tilt acceleration as input in order to be able to control the acceleration threshold in MPC based motion cueing algorithm:

a) otholith's model:

$$\begin{aligned} \dot{x}_{oto} &= A_{oto} \cdot x_{oto} + B_{oto} \cdot u \\ x_{oto} &= [x_{oto1} \quad x_{oto2} \quad x_{oto3} \quad x_{oto4}]^T, \hat{f} = x_{oto1}, u = [\ddot{\theta} \quad u_{acc}] \end{aligned} \quad (3)$$

where:

$$A_{oto} = \begin{bmatrix} -\frac{\tau_L + \tau_S}{\tau_L \tau_S} & 1 & 0 & 0 \\ \frac{1}{\tau_L \tau_S} & 0 & 1 & 0 \\ 0 & 0 & 0 & 1 \\ 0 & 0 & 0 & 0 \end{bmatrix}, B_{oto} = \begin{bmatrix} 0 & \frac{k \cdot \tau_a}{\tau_L \tau_S} \\ 0 & \frac{k}{\tau_L \tau_S} \\ \frac{k \cdot \tau_a \cdot g}{\tau_L \tau_S} & 0 \\ \frac{k \cdot g}{\tau_L \tau_S} & 0 \end{bmatrix}$$

b) semicircular canals' model:

$$\begin{aligned} \dot{x}_{scc} &= A_{scc} \cdot x_{scc} + B_{scc} \cdot u \\ x_{scc} &= [x_{scc1} \quad x_{scc2} \quad x_{scc3} \quad x_{scc4}]^T, \hat{\omega} = x_{scc1}, u = [\ddot{\theta} \quad u_{acc}] \end{aligned} \quad (4)$$

where:

$$A_{scc} = \begin{bmatrix} 0 & 1 & 0 & 0 \\ 0 & -T_2 & 1 & 0 \\ 0 & -T_1 & 0 & 1 \\ 0 & -T_0 & 0 & 0 \end{bmatrix}, B_{scc} = \begin{bmatrix} 0 & 0 \\ T_3 & 0 \\ 0 & 0 \\ 0 & 0 \end{bmatrix}, T_0 = \frac{1}{T_L T_s T_a}$$

$$T_1 = \frac{T_L + T_s + T_a}{T_L T_s T_a}, T_2 = \frac{T_L T_s + T_L T_a + T_s T_a}{T_L T_s T_a}, T_3 = \frac{1}{T_s}$$

By using equations (3) and (4), we can define the system state,  $\hat{x}_k$ , as:

$$\hat{x} = [x_{oto} \quad x_{scc} \quad x_{simu}]^T$$

with  $x_{simu} = [\theta \quad \omega \quad p \quad v \quad \dot{\omega} \quad \dot{v}]^T$

where  $\theta$  represents the tilt angle and  $p$ ,  $x$  or  $y$  position,  $\omega$ ,  $v$  the corresponding velocity.

The state-space model is given:

$$\hat{\dot{x}}_k = \begin{bmatrix} A_{oto} & 0 & 0 \\ 0 & A_{scc} & 0 \\ 0 & 0 & A_{simu} \end{bmatrix} \hat{x}_{k-1} + \begin{bmatrix} B_{oto} & 0 & 0 \\ 0 & B_{scc} & 0 \\ 0 & 0 & B_{simu} \end{bmatrix} \Delta u_{k-1} \quad (5)$$

subject to  $H_m \cdot \hat{x}_k + H_u \cdot \Delta u \leq K$

where  $A_{simu}$  is the simulator's double integrator matrix. For  $N$  step states prediction, using equation (5) as recurrent formulation, we can finally express the quadratic cost function in standard form [Fan3]:

$$\begin{aligned} J_N(X_k) - J_0(x_m, R(k)) &= \frac{1}{2} U^T Q_{U2} U + Q_{U1} U \\ A_u \cdot U &\leq b \\ U &= \begin{bmatrix} \Delta u_1, \Delta u_2, \dots, \Delta u_M, \Delta u_M, \dots, \Delta u_M \end{bmatrix}^T \end{aligned} \quad (6)$$

Based on an efficient QP solver [Kyv1, Fer1], if the system has feasible solution, the input command  $U$  can be solved out. In MPC process, only the first term of optimal solution  $U$  is used. After updating the system with the input command  $\Delta u_1$  and using the next reference signal  $r_{k+1}$ , the calculation process is repeated. This is the basic principle of MPC based motion cueing algorithm. In a real plant system control, the noise disturbances could be important and the model may not be enough accurate to describe the plant physical phenomenon. MPC algorithm can take into account the plant's measurement to correct the model predictive state and perform an offset-free reference tracking by using an integrating disturbance model. The variables in cost function should be shifted by using the steady-state reference values [Pan1]. The principle of MPC algorithm remains the same.

It is found that without any additional restriction, the standard MPC algorithm can lead to some unexpected solutions for slalom test, as illustrated in figure 2:

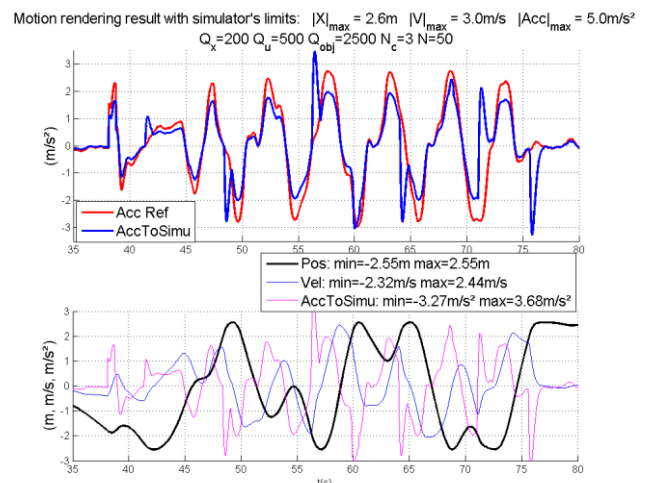


**Fig. 2 Illustration of unexpected solution given by standard MPC algorithm**

In fact, when the motion platform approaches its workspace limit, the simulator must slow down, called also washout process, in order to restrict its motion trajectory within bounds.

Without any additional constraint in motion cueing algorithm, the simulator acceleration could change abruptly or be in opposite direction to the vehicle acceleration with high discrepancy which can provoke a conflicted motion feeling between driver's expectancy, visual and inertial perceptions. By several off-line tuning tests for the scenario, it is possible to find a rather satisfying solution (with  $N=150$  and  $\Delta t=8\text{ms}$  e.g.). But for other scenarios, the tuning parameters are not applicable, not to mention the stability problem. Thus, it is important to develop new MPC-MCA which can ensure a smooth and low discrepancy motion cues during washout process. For this purpose, we have introduced a new system constraint (see below proposed "adaptive" filter) and investigated implicit and explicit MPC algorithms to analyse the performances of existent MPC-MCA.

Another important and difficult issue is how to guarantee the stability of MPC algorithm in all cases. By using the Lyapunov function approach, the stability condition can be described by some explicit terminal set constraints, i.e. that the last predictive state must be steered into the original point or a positively invariant set. Generally, two well-known explicit terminal set conditions are adopted: the first is a zero terminal set stability condition, the second, with more large feasible solution domain is the LQR terminal set condition in which the LQR control law is completely available [Bem1]. Authors' study showed that in real-time system, the MPC algorithm using these standard conditions is efficient only if the system is 1DOF motion rendering problem. For a 2, 3DOF motions cueing problem, a limited area of feasible solutions was found [Fan2], otherwise, as used by Dagdelen et al., Augusto and Garrett et al., the stability condition must be relaxed. To improve the efficiency of MPC-MCA with perceived motion threshold control in washout process, a new system's constraint is proposed by authors, which can not only guarantee the system's stability but also keep a smoothing washout transition. This condition is expressed by the following equation:

$$x_i(t) + c_v \cdot v_i(t) \cdot T + c_u \cdot u_i(t) \cdot T^2/2 = x_{max} \quad (7)$$

where  $x$ ,  $v$ ,  $u$  are respectively the simulator's position, velocity and acceleration and  $x_{max}$ , the simulator's excursion limit.

If the equality condition is detected in-line with current state value, the system must be slowed down.

The equation (7) can be written in Laplace-transform space as follows [Fan3]:

$$x_i(s) = \frac{x_0}{s} + \frac{v_0 + \omega_n^2(x_{max} - x_0)/s}{(s^2 + 2\xi \cdot \omega_n \cdot s + \omega_n^2)} \quad (8)$$

where the natural frequency  $\omega_n = [2/(c_u \cdot T^2)]^{0.5}$  and the damping ratio:  $\xi = c_v/(2 \cdot c_u)^{0.5}$ ,  $x_0$  and  $v_0$  are the last simulator state from which the braking process or washout process is engaged. From (8), we can find that the position,  $x_i(s)$ , is composed of an offset,  $x_0$ , a second order system homogenous response and a step response with amplitude  $(u_0 + 2\xi \cdot \omega_n \cdot v_0)$ . The characteristics of second order system [Row1] show that the response feature of  $x_i(s)$  is determined by the system's natural frequency and damping coefficient. Assuming that the damping ratio is superior to 1, the maximum value of  $x_i(t)$  is equal to  $x_{max}$ . As a consequence, the workspace constraint condition is fulfilled at all times and the washout motion's acceleration is completely controlled by the system parameters. Recall that if the system (8) is underdamped, it can produce an overshoot value which can, in some cases, be benefit to motion rendering results. If the underdamped strategy is used, the overshoot value should be taken into account in the limitation of workspace consequently.

Note that in the classical filter approach, a 2e order HP filter is applied to limit the simulator excursion:

$$G_{HP}(s) = \frac{u_s(s)}{u_{veh}(s)} = \frac{k \cdot s^2}{(s^2 + 2\xi \cdot \omega_{n1} \cdot s + \omega_{n1}^2)} \quad (9)$$

where  $k/\omega_{n1}^2 < x_{max}/u_{step}$  and:

for *small.simulator.stroke*:  $\omega_{n1} = 2.5 - 4$ ,  $\xi = 1 - 1.4$

for *big.simulator.stroke*(Renault, PSA.etc.):  $\omega_{n1} = 0.7 - 1$ ,  $\xi = 0.7 - 1.4$

The HP filter's parameters must be designed at worst case, i.e. the step signal for which the maximum stroke is required. Another disadvantage of classical filter is the backlash effect produced at the end of acceleration or

braking signal (cf. fig. 3) which is very difficult to be fully compensated by the tilt motion and causes often the artifacts effect or simulator sickness [Rey1]. Compared with relation (9), the corresponding acceleration HP filter of relation (8) can be rewritten as [Fan3]:

$$G_{HP2}(s) = \frac{u_s(s)}{u_0/s} = \frac{\left[1 - \frac{\omega_n^2 (v_0/u_0)}{s}\right] s^2}{(s^2 + 2\xi\omega_n s + \omega_n^2)} \quad (10)$$

which can be considered as a special explicit adaptive filter with filter's gain taking into account the evolution of simulator state. If we fixed  $c_v = 1$ , and  $c_u = 0.45$ , we have only one parameter T to consider. In this case, the reasonable value of T deduced by simulation experiences is between 0.8 to 3, and thus leads to  $\omega_n = 0.7$  to 3.0. The figure 3 illustrates the classical filter and proposed "adaptive" filter's results for the rectangular pulse reference signal.

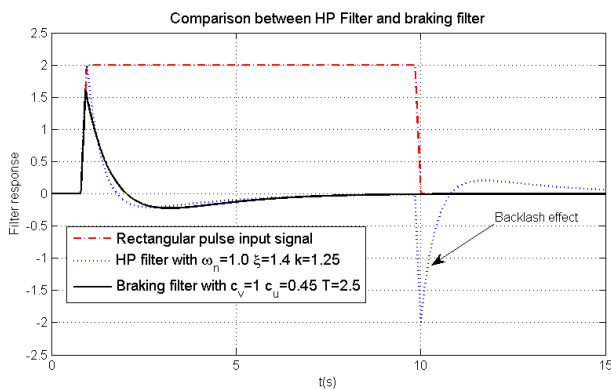


**Fig. 3 Comparison of filters results between classical HP filter and proposed filter**

According to the filters results presented in figure 3, we can find that the backlash effect is completely removed by using the proposed filter (10). The relation (7) is a linear combined expression of state variables. It is easy to integrate, as system constraint, in MPC model.

### 3. Influence of vestibular system and tuning process description

#### 3.1. Tuning process description

Before addressing the topic of vestibular model's influence in the MPC algorithm, we describe at first the tuning method and the used tuning signal, a rectangular pulse. Not only it is simple, but also it is very close to the braking

deceleration measurement. Compared with the acceleration or deceleration signal in full throttle or gas pedal releasing manoeuvres, both accelerations are similar too, but not for deceleration caused by the natural vehicle resistance forces (aerodynamic force, rolling resistant force, powertrain force). The slope of deceleration at the end of the rectangular pulse is steeper than that of vehicle's natural deceleration. So it is a severe motion rendering signal. Hence, if we can get a satisfactory tuning result for this basic signal, the tuning task for a general purpose driving test is almost achieved.

By choosing the different weighting coefficient or matrices, 8 coefficients in total with 2 additional constants  $T_x$  and  $T_\theta$ , a rather good trade-off result is obtained within the required system constraints (cf. fig. 4). Once the step signal tuning is realized, the position weighting parameter can afterwards be adjusted to enhance the washout occurrence for the general driving tests. The motion cueing algorithm is then tested in Renault's 8DOF driving simulator. A satisfactory driving simulator feeling is obtained from normal drivers as well as internal professional drivers.

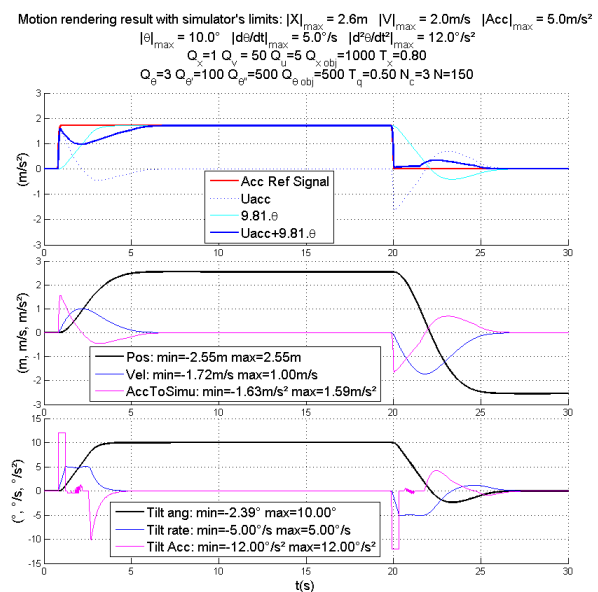


**Fig. 4: 2DOF motion rendering result using MPC ideal simulator's model for rectangular pulse**

In practice, the tilt threshold control is a more complex issue. As reported by [Cha1], the threshold can be raised if a linear motion occurs simultaneously. In addition, vehicle's

pitch rate or pitch acceleration can be higher than the conventional tilt thresholds in some short lapse of time. These two factors are also considered in our MPC algorithm to have an optimal tilt motion. The accurate dynamic thresholds will be quantified in our future experiences for the restitution of longitudinal motion.

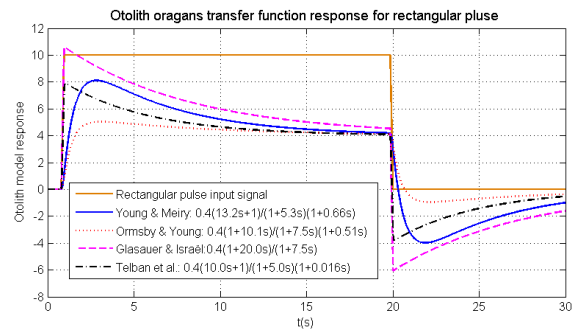
**3.2. Using vestibular model or not**

The integration of vestibular system in the MPC state-space model aims at approaching as close as possible the perceived inertial force and rotational rate between a real car and the simulator virtual environment. From a scientific standpoint, it could improve the efficiency of motion cueing algorithm if the models are representative of the human vestibular system. In fact, we have used the model’s dynamic and dead-detection features to optimize the washout process or the motion cues. As reported by Chen et al. [Che1], when the reference signal is below some threshold, a washout process is automatically started. This simple strategy can improve motion cueing efficiency due to more exploitable simulator excursions. But the use of such threshold can unfortunately increase the system’s delay and disturb more or less the delay compensation function if it is implemented. It is a method suitable for relatively calm motion situation. The washout algorithm based on the vestibular dynamic feature, as studied in a fight simulator [Tel1] firstly, reveals its potential advantages for general purposes. However, the evaluation of benefic using vestibular model is not so obvious without experimental tests. In fact, the motion cueing result depends on in some ways the used parameters of vestibular model. We report in table 1, some typical transfer functions of vestibular system. The convolution results between the transfer functions and the rectangular pulse signal demonstrate that not all the dynamic features given by various vestibular models are similar. The perceived specific force evaluated by using Telban’s otoliths model is similar to that of Glasauer & Israël. These two models have more large frequency bandwidth than others. Young and Ormsby’s otoliths models have more LP filter feature and give smoother response signal than the two previous

ones. Figure 5 shows that the high frequency bandwidth otoliths’ models give a filter result close to the ideal simulator’s one for a fast change signal. But for the final response of a steady specific force, the perceived value is about twice lower than the beginning for the rectangular pulse signal. It is probably the area that we can exploit to optimize the washout process with some allowed tracking error. So it would be a useful work to compare the motion rendering results given by incorporating or not the vestibular model in motion cueing algorithm.

**Table 1. Human vestibular model parameters [Tel1]**

$\frac{\hat{f}}{f} = \frac{k(\tau_a \cdot s + 1)}{(\tau_L \cdot s + 1)(\tau_s \cdot s + 1)}$				
Parameter	Young & Meiry (1968)	Ormsby (1974)	Glasauer & Israël (1995)	Telban et al. [7]
$\tau_a$	5.3	7.5	7.5	5.0
$\tau_l$	0.66	0.51	0.0	0.016
$\tau_s$	13.2	10.1	20.0	10
k	0.4	0.4	0.4	0.4
Threshold, $d_{TH}$ (m/s <sup>2</sup> )	Sway = 0.17 Surge = 0.17 Heavy = 0.28 [16]			
$\frac{\hat{\omega}}{\omega} = \frac{k_{sc} T_L T_a s^2 (1 + T_b \cdot s)}{(T_L \cdot s + 1)(T_s \cdot s + 1)(T_a \cdot s + 1)}$				
Parameter	Ormsby & Young (1977)	Reid & Nahon [16]	Reid & Nahon [16]	Telban et al. [7]
$T_L$	18	6.1 (Roll)	5.3 (Pitch) 10.2 (Yaw)	5.73
$T_s$	0	0.1	0.1	0.005
$T_a$	30	30	30	80
$T_b$	0	0	0	0.06
$k_{sc}$	1.0	1.0	1.0	28.65
Threshold	Pitch=2.0°/s Roll = 2.0°/s Yaw = 1.6°/s [16]			



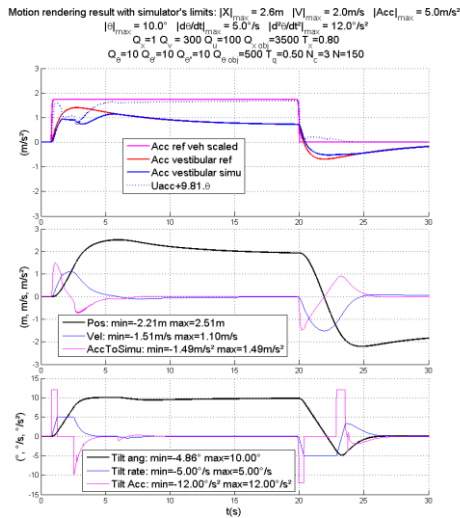
**Fig. 5: Comparison of dynamic features given by various otoliths’ models**

Figure 6 illustrates that a motion rendering result obtained from Young & Meiry otoliths model can give high frequency false cues. It is consistent with the result presented in figure 5. Naturally, using  $\Delta u$  as input MPC control, the

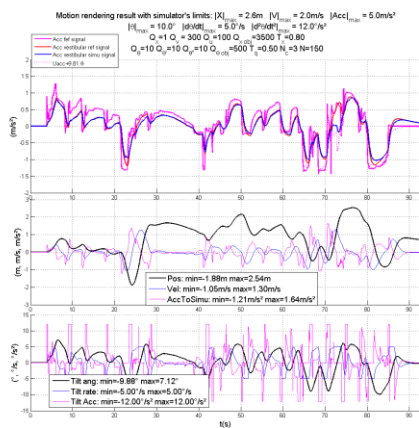
corresponding state variable  $u$  can be regulated more smoothly in MPC algorithm.

Figure 7 illustrates an experience's test result. A good feedback is obtained from normal and professional drivers. Note that, in this test, the vertical acceleration plays also a non negligible role for the fidelity of driving simulation.

The professional drivers remarked also the benefice of hexapod linear motion to enhance the longitudinal acceleration feeling. One of the developed MPC 3DOF motion cueing algorithm structures not detailed here is very similar to that in classical filter [Fis1].



**Fig. 6: 2DOF motion rendering result using vestibular models for rectangular pulse**



**Fig. 7: 2DOF motion rendering result using vestibular models for longitudinal acceleration**

### 4. Pre-position technique and vehicle motion prediction

The figure 4 shows that a good agreement is generally obtained by using MPC based motion

cueing algorithm. However, if we focus on the first fraction of motion rendering result, we can observe that there is a lack of linear acceleration level in specific force 2 seconds after tracking the reference signal. We can also observe that the falling signal tracking at the end of rectangular pulse is well achieved. In fact, the different motion rendering results of these two similar reference signals can be explained by the available rail length. In the beginning, the simulator is in its neutral position. We have 2.6m rail stroke, at the end, double available distance. If a pre-position technique is carried out just before the desired event, the motion rendering result will be better. By using the pre-position technique, a simulated result presented in fig. 8 confirms the preceding analysis. Compared with the motion rendering result reported in fig. 4, we can find the crucial role played by this technique. For this purpose, a bang-bang motion control algorithm (time minimization algorithm) which can be activated in-line by scenario is developed in Renault's driving simulator. Once the optimal position is reached, by means of detecting some trigger signal, e.g. a fast velocity change from pedal, the MPC algorithm takes the motion cueing task immediately. Note that the senseless pre-position motion must be controlled under the perceived threshold. It takes about 7-15s to reach the optimal position for the ULTIMATE. The benefice given by pre-position technique leads us to think naturally our future development to incorporate a driver's model in order to predict oncoming trajectory. For MPC based driver model, using road information, imposed velocity range, acceleration limit and vehicle's dynamic model, a vehicle motion prediction is possible. As presented by LMS and VI-Grade, the MPC algorithm can already forecast a right vehicle trajectory using 40-50m of forward road information. Using this technique to predict the vehicle's acceleration or deceleration could be helpful to accomplish the pre-position task. However, the driver's small random action on vehicle's command (steering-wheel, gas pedal or brake) can completely change the simulator's trajectory. It is important to set appropriated threshold to filter any undesired manoeuvre.

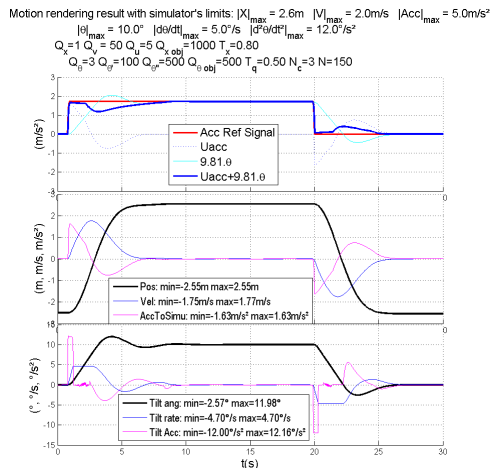


**Fig. 8: 2DOF motion rendering result with help of pre-position technique**

### 5. Evaluation of simulators potential performances based on motion cueing algorithm

One of important questions to build X, Y rails based simulator is that what is the optimal rail stroke to achieve a desired specific force or acceleration tracking task? Based on ULTIMATE actuators’ performances and others, we have compared here simulators performances using three scenarios. The first is the 0.2Hz slalom manoeuvre in scale 1:1 or an artificially amplified acceleration signal, the second, a scaled emergency braking signal limited to 5m/s<sup>2</sup>, and the last, a general starting braking scenario. The reason to limit the deceleration level to 5m/s<sup>2</sup> for the emergency braking is given as below:

- the tilt angle can’t exceed 30° without perceived tilt cockpit position (Aubert effect[Rey1]).
- the limitation on rail stroke and tilt rate makes the full specific force signal tracking difficult, even impossible in the case of tracking a sustained acceleration signal superior to 5m/s<sup>2</sup>.

Note that, for the slalom test, the higher the slalom frequency, the higher the lateral acceleration which can be reproduced by linear motion if the simulator’s frequency bandwidth allows to. For the 0.2Hz slalom test, only 1DOF motion cueing results are compared.

The table 3 summarizes the simulated potential performances.

**Table 3: Simulators performances evaluated by 1DOF and 2DOF MPC based motion cueing algorithm**

Scenario	0.2Hz slalom / 1DOF	emergency braking for 5s(>5m/s <sup>2</sup> ) / 2DOF	starting & braking longitudinal cues <sup>(b)</sup> / 2DOF
ULTIMATE	2.8m/s <sup>2</sup>	1.7m/s <sup>2</sup>	1.8m/s <sup>2</sup>
DAIMLER	7.5m/s <sup>2</sup>	2.5m/s <sup>2</sup>	3m/s <sup>2</sup>
TOYOTA*	6m/s <sup>2</sup>	5m/s <sup>2</sup> (a)	5m/s <sup>2</sup>

\*Assumption: available stroke X=35m, Y=20m, V≤6m/s, Acc≤6.5m/s<sup>2</sup>; (a): in limited acceptance (b) 2-3s events

It can be found from table 3 that the simulators lateral performances could be high for slalom test, while the longitudinal performances, rather limited to 5m/s<sup>2</sup> for sustained acceleration or deceleration. Note that, if the event takes place in short duration, the combined rail and hexapod linear acceleration can reach very high performance. This situation is not compared here.

### 6. Conclusion

In this paper, the Renault’s latest MPC based motion cueing algorithm theory and practices have been reviewed. The proposed system stable condition is emphasized by a comprehensive physical mean and can be considered as a special adaptive filter. It doesn’t need to steer again the last predictive step into a positively invariant set, because it is [Fan2]. Beside of its important role played in the algorithm’s stability, another one is its capability to reduce the predictive step length’s influence on the motion cueing results. It thus enhances significantly the efficiency of MPC-MCA with motion threshold control in washout process. Using this condition, we have developed both explicit and implicit MPC-MCA. The former is more robust for algorithm implementation and the later, more flexible and more powerful is suitable for handling high complex-system and also for performing off-line simulation, tuning task. However, the iteration-limit set in the QP solver due to the on-line requirement could make the implicit MPC algorithm unstable [Mor1]. Even if it is a very low probability event, specific safety algorithm needs to be implemented to prevent from motion cueing algorithm’s crash in high performance simulators.

## 7. References

- [Alq1]** Al Qaisi I., A. Traechtler, "Constrained Linear Quadratic Optimal Controller for Motion Control of ATMOS Driving Simulator", DSC Europe 2012 proceedings, Paris, France
- [Aug1]** Augusto B.D.C., "Motion Cueing in the Chalmers Driving Simulator: An Optimization-Based Control Approach", Master of Science Thesis, 2009
- [Beg1]** Beghi A., M. Bruschetta, F. Maran, D. Minen "A Model-based Motion Cueing strategy for compact driving simulation platforms", DSC Europe 2012 proceedings, Paris, France
- [Bem1]** Bemporad A. and M. Morari, "Robust Predictive Control: A Survey", *Robustness in Identification and Control*, vol. 245, pp. 207-226, 1999
- [Cha1]** Chapron T., Colinot J.P., "The new PSA Peugeot-Citroën Advanced Driving Simulator – Overall design and motion cue algorithm", DSC North America 2007 proceedings, Iowa City
- [Che1]** Chen S.H., and Li-Chen Fu, "An Optimal Washout Filter Design for a Motion Platform with Senseless and Angular Scaling Maneuvers", *American Control Conference (ACC)*, 2010: Baltimore, Maryland, USA, 30 June - 2 July 2010
- [Dag1]** Dagdelen M., G. Reymond, A. Kemeny, M. Bordier, and N. Maýzi (2004). "MPC based motion cueing algorithm : Development and application to the ULTIMATE driving simulator", DSC Europe 2004 proceedings, pp. 221-233, Paris, France
- [Fan1]** Fang Z., A. Kemeny. "Motion cueing algorithms for a real-time automobile driving simulator", DSC Europe 2012 proceedings, pp. 159-174, Paris, France
- [Fan2]** Fang Z., A. Kemeny. "Explicit MPC motion cueing algorithm for real-time driving simulator", *IPEMC 2012 (June-2-5 2012) Harbin, China Vol. 2 (2012) 874-878*
- [Fan3]** Fang Z., A. Kemeny. "An efficient MPC based motion cueing algorithm to driving simulator", Internal report, Renault, May 2014
- [Fan4]** Fang Z., G. Reymond, A. Kemeny, "Performance identification and compensation of simulator motion cueing delays", DSC Europe 2010 proceedings, Paris, France
- [Fer1]** H.J. Ferreau and H.G. Bock and M. Diehl, "An online active set strategy to overcome the limitations of explicit MPC", *International Journal of Robust and Nonlinear Control*, 2008, vol. 18, N°8, pp.816–830
- [Fis1]** Fischer M., Sehammer H. and Palmkvist G., "Motion cueing for 3-, 6- and 8-degrees-of-freedom motion systems", DSC Europe 2010 proceedings, Paris, France
- [GAR1]** Garrett N.J.I., M. C. Best, "Model predictive driving simulator motion cueing algorithm with actuator-based constraints", *Vehicle System Dynamics: International Journal of Vehicle Mechanics and Mobility* Vol.51, Issue8, (2013) 1151-1172
- [Kva1]** M. Kvanisca, "Real-Time Model Predictive Control via Multi-Parametric Programming: Theory and Tools, VDM Verlag, 2009
- [Mor1]** Morari M. & Jones C. et al., "Real-time optimization for distributed model predictive control", 2010, Automatic control Laboratory, ETH Zürich
- [Oma1]** Oman C.M., 1990, "Motion sickness: a synthesis and evaluation of the sensory conflict theory", *Can J Physiol Pharmacol* 68(2), 294-303
- [Pan1]** Gabriele Pannocchia, "Course on Model Predictive Control Part II – Linear MPC design", University of Pisa, Italy, July 2012
- [Row1]** Rowell D., "Review of First- and Second-Order System Response", (2004), MIT, [web.mit.edu/2.151/www/Handouts/FirstSecondOrder.pdf](http://web.mit.edu/2.151/www/Handouts/FirstSecondOrder.pdf)
- [Siv1]** Sivan R., Ish-Shalom J., and Huang J. K., "An Optimal Control Approach to the Design of Moving Flight Simulators", *IEEE Transactions on Systems, Man, and Cybernetics*, 1982. 12(6): p. 818-827
- [Sor1]** Olof Sörnmo and Anna Lindholm, "An Evaluation of the Development of Different Areas within Automatic Control over the Years", May, 2012 [http://www.control.lth.se/media/Education/DoctorateProgram/2012/HistoryOfControl/Anna\\_Olof-SomeFields-rep.pdf](http://www.control.lth.se/media/Education/DoctorateProgram/2012/HistoryOfControl/Anna_Olof-SomeFields-rep.pdf)
- [Tel1]** Telban Robert J. and Frank M. Cardullo, "Motion Cueing Algorithm Development: Human-Centered Linear and Nonlinear Approaches", NASA /CR-2005-213747